COMMUNICATIONS IN NUMERICAL METHODS IN ENGINEERING
Commun. Numer. Meth. Engng 2003; **19**:275–284 (DOI: 10.1002/cnm.588)

A second order discontinuous Galerkin method for advection on unstructured triangular meshes

H. J. M. Geijselaers*,† and J. Huétink

Mechanical Engineering, University of Twente, P.O. Box 217, 7500 AE Enschede, The Netherlands

SUMMARY

In this paper the advection of element data which are linearly distributed inside the elements is addressed. Across element boundaries the data are assumed discontinuous. The equations are discretized by the Discontinuous Galerkin method. For stability and accuracy at large step sizes (large values of the Courant number), the method is extended to second order. Furthermore the equations are enriched with selective implicit terms. This results in an explicit and local advection scheme, which is stable and accurate for Courant numbers less than .95 on unstructured triangle meshes. Results are shown of some pure advection test problems. Copyright © 2003 John Wiley & Sons, Ltd.

KEY WORDS: linear advection; discontinuous Galerkin; finite elements

1. INTRODUCTION

In this note we study the transient evolution of a data field $f(\mathbf{x},t)$, which is governed by the scalar advection equation.

$$\frac{\partial f}{\partial t} + \mathbf{a}\cdot\nabla f \tag{1}$$

$\mathbf{a}(\mathbf{x})$ is the advective velocity. The advection equation is discretized using finite elements. The discretized field $f_h(\mathbf{x},t)$ is assumed discontinuous across element boundaries.

The method as presented in this paper has been developed for use in the Arbitrary Lagrangian Eulerian (ALE) method in solid mechanics [1–3]. Other applications may be in the field of fluid mechanics, such as pollution transport [4], sub sonic and supersonic aerodynamics [5–7] or visco-elastic flow [8, 9].

Equation (1) is discretized using the Discontinuous Galerkin method [10]. The Discontinuous Galerkin Method and the extensions as proposed in this paper will be demonstrated on the one dimensional advection equation in Section 2. Generalization to the multi-dimensional case is shown in Section 3.

*Correspondence to: H. J. M. Geijselaers, Department of Mechanical Engineering, University of Twente, P.O. Box 217, 7500 AE Enschede, The Netherlands
†E-mail: h.j.m.geijselaers@wb.utwente.nl

Received 14 May 2001
Accepted 20 July 2002

2. ONE DIMENSIONAL ADVECTION

We want to solve for $f(x,t)$, $(x\in[0,L];\ t\in[0,T])$, such that

$$\frac{\partial f}{\partial t}+a\frac{\partial f}{\partial x}=0 \qquad f(0,t)=f_0 \quad \text{and} \quad f(x,0)=F(x) \tag{2}$$

The time axis $[0,T]$ is partitioned into N_t intervals $[t_{i-1},t_i]$, where $i\in[1,N_t]$. A deferred task is to construct the solution at $t=t_i$ based on the distribution at $t=t_{i-1}$.

In literature increments at finite time steps are typically obtained by time integration.

$$\Delta f_i=\int_{t_{i-1}}^{t_i}\frac{\partial f}{\partial t}\,\mathrm{d}t \tag{3}$$

For accuracy high order time integration is used, e.g. a Taylor Galerkin approach [9] or second or third order Runge–Kutta [5]. For stability and monotonicity often limiters are employed [4, 5].

Instead of integrating in time, we will regard the advection equation as a projection in space. We assume that we know the advective displacement c rather than the advective velocity.

$$c=(t_i-t_{i-1})a \tag{4}$$

In that case we can calculate the convective increment $\Delta f_i(x)$ straight away.

$$\Delta f_i(x)=f(x,t_i)-f(x,t_{i-1})=f(x-c,t_{i-1})-f(x,t_{i-1}) \tag{5}$$

The increment Δf is written by means of Taylor expansion in x as

$$\Delta f(x)=-c(x)\frac{\partial f}{\partial x}+\frac{1}{2}(c(x))^2\frac{\partial^2 f}{\partial x^2}+O(c^3) \tag{6}$$

For conservation type equations a similar approximation can be derived [11, 12].

2.1. The second order discontinuous Galerkin method

The spatial domain $[0,L]$ is partitioned into N_x intervals $I_n=[x_{n-1},x_n]$, where $n\in[1,N_x]$. The field f as well as the increment Δf are discretized on I_n using discontinuous base functions $w_n(x)$ (Figure 1).

$$f_h^n(x,t)=\sum_k w_n^k(x)f_k^n(t) \qquad \Delta f_h^n(x)=\sum_k w_n^k(x)\Delta f_k^n \tag{7}$$

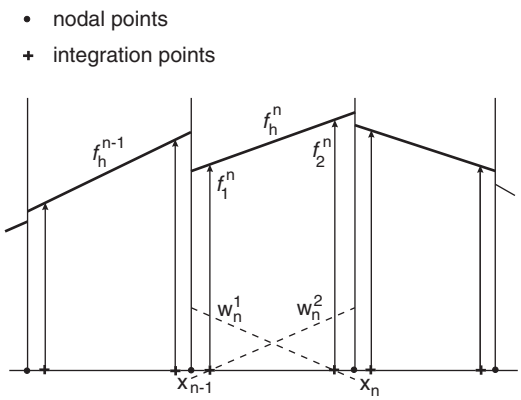

Figure 1. Discontinuous function discretization on I_n.

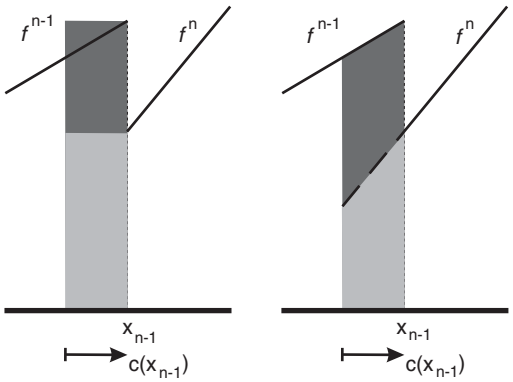

Figure 2. First order vs second order boundary flux.

The second order expansion (6) for the increment Δf^n on I_n is written in a weak form.

$$\int_{x_{n-1}}^{x_n} \Delta f_h^n(x) w_n^k \, \mathrm{d}x = -\int_{x_{n-1}}^{x_n} \left(c(x)\frac{\partial f_h^n}{\partial x} - \frac{1}{2}c(x)^2 \frac{\partial^2 f_h^n}{\partial x^2} \right) w_n^k \, \mathrm{d}x \quad \forall w_n^k \tag{8}$$

The f_h-field is assumed discontinuous across interval boundaries. We follow [10] and weakly enforce continuity of f at the inflow boundary x_{n-1}. We deal with a finite step, therefore we enforce continuity during the whole time step $[t_{i-1}, t_i]$.

$$\begin{aligned}\int_{x_{n-1}}^{x_n} \Delta f_h^n w_n^k \, \mathrm{d}x = &-\int_{x_{n-1}}^{x_n} \left(c\frac{\partial f_h^n}{\partial x} - \frac{1}{2}c^2 \frac{\partial^2 f_h^n}{\partial x^2} \right) w_n^k \, \mathrm{d}x \\ &- \int_{t_{i-1}}^{t_i} a(x_{n-1}) w_n^k(x_{n-1}) (f_h^n(x_{n-1}, t) - f_h^{n-1}(x_{n-1}, t)) \, \mathrm{d}t \quad \forall w_n^k \end{aligned} \tag{9}$$

Using (2) a second order approximation to the boundary term is derived.

$$\begin{aligned}\int_{t_{i-1}}^{t_i} a(x_p) w_q(x_p) f(x_p, t) \mathrm{d}t &\approx a(x_p) w_q(x_p) \int_{t_{i-1}}^{t_i} \left(f(x_p, t_{i-1}) + (t - t_{i-1}) \frac{\partial f}{\partial t} \right) \mathrm{d}t \\ &= a(x_p) w_q(x_p) \int_{t_{i-1}}^{t_i} \left(f(x_p, t_{i-1}) - (t - t_{i-1}) a(x_p) \frac{\partial f}{\partial x} \right) \mathrm{d}t \\ &= c(x_p) w_q(x_p) \left(f(x_p, t_{i-1}) - \frac{1}{2} c(x_p) \frac{\partial f}{\partial x} \right) \end{aligned} \tag{10}$$

This result is illustrated in Figure 2. Substitution into (9) yields

$$\int_{x_{n-1}}^{x_n} \Delta f_h^n w_n^k \, \mathrm{d}x = -\int_{x_{n-1}}^{x_n} \left(c\frac{\partial f_h^n}{\partial x} - \frac{1}{2}c^2 \frac{\partial^2 f_h^n}{\partial x^2} \right) w_n^k \, \mathrm{d}x$$

$$- c(x_{n-1})w_n^k(x_{n-1})\left(f_h^n(x_{n-1},t_{i-1}) - \frac{1}{2}c(x_{n-1})\frac{\partial f_h^n}{\partial x}\right)$$
$$+ c(x_{n-1})w_n^k(x_{n-1})\left(f_h^{n-1}(x_{n-1},t_{i-1}) - \frac{1}{2}c(x_{n-1})\frac{\partial f_h^{n-1}}{\partial x}\right) \quad \forall w_n^k \quad (11)$$

After partial integration the jump term at the inflow boundary splits up into two flux terms, an influx from the upwind element and an out-flux at the outflow boundary.

$$\int_{x_{n-1}}^{x_n} \Delta f_h^n w_n^k \,\mathrm{d}x = \int_{x_{n-1}}^{x_n} \left(\frac{\mathrm{d}(cw_n^k)}{\mathrm{d}x} f_h^n - \frac{1}{2}\frac{\mathrm{d}(c^2 w_n^k)}{\mathrm{d}x}\frac{\partial f_h^n}{\partial x}\right)\mathrm{d}x$$
$$+c(x_{n-1})w_n^k(x_{n-1})\left(f_h^{n-1}(x_{n-1},t_{i-1}) - \frac{1}{2}c(x_{n-1})\frac{\partial f_h^{n-1}}{\partial x}\right)$$
$$- c(x_n)w_n^k(x_n)\left(f_h^n(x_n,t_{i-1}) - \frac{1}{2}c(x_n)\frac{\partial f_h^n}{\partial x}\right) \quad \forall w_n^k \quad (12)$$

Δf is solved for on an element by element basis. When discretized using a linear interpolation per element, based on function values in Gauss integration points the 'mass' matrix in the left hand side of Equation (12) is diagonal.

Equation (12) is equivalent to the result of the two step procedure of Reference [4], which is derived from a first order discretization. The presentation as in Equation (12) shows, that improved stability stems from the second order boundary fluxes as well as from a (naturally arising) diffusion term $(1/2)c^2(\partial^2 f/\partial x^2)$. In 2D or 3D this term takes the form of stream-line diffusion.

2.2. *Element-wise point-implicit scheme*

The scheme of Equation (12) is stable for Courant numbers $(Cr) < 0.7$ (see Figure 6). For many applications this is already sufficient. To extend the stability region we follow [6] and apply an element-wise point-implicit scheme. To this end implicit terms are added to selected terms coming from weight functions, whose support is the domain of one element, with respect to the degrees of freedom associated with that same element.

$$\int_{x_{n-1}}^{x_n} \Delta f_h^n w_n^k \,\mathrm{d}x = \int_{x_{n-1}}^{x_n} \left(\frac{\mathrm{d}(cw_n^k)}{\mathrm{d}x}(f_n^h + \alpha\Delta f_h^n) - \frac{1}{2}\frac{\mathrm{d}(c^2 w_n^k)}{\mathrm{d}x}\frac{\partial(f_n^h + \beta\Delta f_h^n)}{\partial x}\right)\mathrm{d}x$$
$$+c(x_{n-1})w_n^k(x_{n-1})\left(f_h^{n-1}(x_{n-1},t_{i-1}) - \tfrac{1}{2}c(x_{n-1})\frac{\partial f_h^{n-1}}{\partial x}\right)$$
$$-c(x_n)w_n^k(x_n)\left(f_h^n(x_n,t_{i-1}) - \tfrac{1}{2}c(x_n)\frac{\partial f_h^n}{\partial x}\right) \quad \forall w_n^k \quad (13)$$

Note that the implicit terms are only added to the terms in the integral. Adding these terms to the f_h^n terms at the outflow boundary x_n, as is proposed in Reference [6], will make the method non-conservative. When this is remedied by also adding implicit terms to the f_h^{n-1} terms at the inflow boundary, again a conservative method is obtained but then the local character is lost.

Numerical experiments indicate that $\alpha = -1/60$ and $\beta = 2/3$ is a good choice. A priori it may be expected that the β-term will have a stabilizing effect. This term adds an additional (stream line) diffusion within each element. A small negative value for α seems to prevent the system from being overly damped.

Although after collecting all terms with Δf in the left hand side, the 'mass' matrix is neither diagonal nor symmetric anymore, it remains local. The preferred explicit element by element solution is still possible.

3. MULTI DIMENSIONAL ADVECTION

In two (or three) dimensions Equation (6) is written as

$$\Delta f = -\mathbf{c}\cdot\nabla f + \tfrac{1}{2}\mathbf{cc}:\nabla\nabla f + O(\mathbf{c}^3) \tag{14}$$

The domain is divided into non-overlapping triangles or quadrilaterals, on which f and Δf are discretized in a way similar to Equation (7) to obtain a linear distribution in each element. Equation (14) is written in the weak form while weakly enforcing continuity over the inflow boundary to obtain the counterpart of Equation (11).

$$\int_{V_n} w_n^k \Delta f_h^n \,\mathrm{d}V = -\int_{V_n} w_n^k \mathbf{c}\cdot(\nabla f_h^n - \tfrac{1}{2}(\nabla\nabla f_h^n)\cdot\mathbf{c})\,\mathrm{d}V + \int_{\Gamma_n^-} w_n^k \mathbf{c}\cdot\mathbf{n}(f_h^n - f_h^{n(-)} - \tfrac{1}{2}\mathbf{c}\cdot(\nabla f_h^n - \nabla f_h^{n(-)}))\,\mathrm{d}\Gamma \quad \forall w_n^k \tag{15}$$

Here Γ_n^- is defined as that part of the boundary of the nth element where $\mathbf{c}\cdot\mathbf{n} < 0$, where $\mathbf{n}$ is the outward pointing normal. $f_h^{n(-)}$ is the value of f in the elements which share boundaries Γ_n^- with the nth element.

After partial integration the terms with α and β are added like in Equation (13) and all terms containing Δf are collected in the left hand side.

$$\begin{aligned}\int_{V_n} (w_n^k \Delta f_h^n - \alpha\nabla\cdot(w_n^k\mathbf{c})\Delta f_h^n + \tfrac{1}{2}\beta\nabla\cdot(w_n^k\mathbf{cc})\cdot\nabla\Delta f_h^n)\,\mathrm{d}V \\ = \int_{V_n} (\nabla\cdot(w_n^k\mathbf{c})f_h^n - \tfrac{1}{2}\nabla\cdot(w_n^k\mathbf{cc})\cdot\nabla f_h^n)\,\mathrm{d}V - \int_{\Gamma_n^-} w_n^k\mathbf{c}\cdot\mathbf{n}(f_h^{n(-)} - \tfrac{1}{2}\mathbf{c}\cdot\nabla f_h^{n(-)})\,\mathrm{d}\Gamma \\ - \int_{\Gamma_n^+} w_n^k\mathbf{c}\cdot\mathbf{n}(f_h^n - \tfrac{1}{2}\mathbf{c}\cdot\nabla f_h^n)\,\mathrm{d}\Gamma \quad \forall w_n^k\end{aligned} \tag{16}$$

where Γ_n^+ is defined as $(\Gamma_n^+ \cup \Gamma_n^- = \Gamma_n,\ \Gamma_n^+ \cap \Gamma_n^- = \emptyset)$.

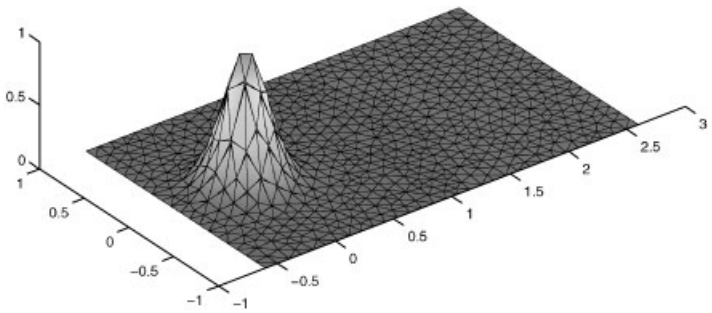

Figure 3. Advection of a Gaussian bump, initial distribution.

3.1. Implementation

Equation (16) has been implemented for 3-node triangular 2-D elements. The displacement field is C_0-continuous and piece wise linear. The interpolation of element data f is linear and discontinuous over element boundaries. Inspection of Equation (16) shows that the boundary flux terms are of degree 3. The volume integrals involve polynomials of degree 2.

We choose to evaluate the boundary flux integrals as accurately as possible. Two integration points per edge are used for evaluation of the fluxes. Three integration points are used to evaluate the volume integrals.

4. SIMULATIONS

The proposed method will be demonstrated on simulations of pure advection with a constant and a varying velocity field.

4.1. Advection of a Gaussian bump

The objective of this series of calculations is to asses the stability and accuracy of the method. A rectangle of size 2×3.2 is divided into 1318 elements. The initial value of the field to be convected is a discontinuous least squares approximation of a Gaussian bump (Figure 3).

$$f = 0.01^{4(x^2+y^2)} \tag{17}$$

This bump is convected over a distance of 2 in x-direction. In Figure 4 the final distribution is shown when the advection is done in 81 steps. The maximum Courant number in any element is 0.95. The Courant number is defined as

$$Cr_n = \frac{1}{2V_n} \int_{\Gamma_n} \|\mathbf{c} \cdot \mathbf{n}\| \, \mathrm{d}\Gamma; \quad Cr_{\max} = \max(Cr_n) \tag{18}$$

In Figure 5 the evolution of the maximum and minimum values of the nodal averaged f is given. No instabilities are visible. The maximum value remains close to 1, while there is no undershoot. The error in the phase velocity is less than 10^{-5}.

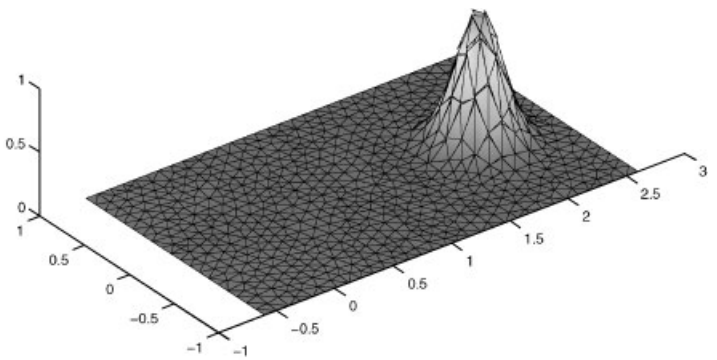

Figure 4. Advection of a Gaussian bump, final profile ($Cr_{\max} = 0.95$).

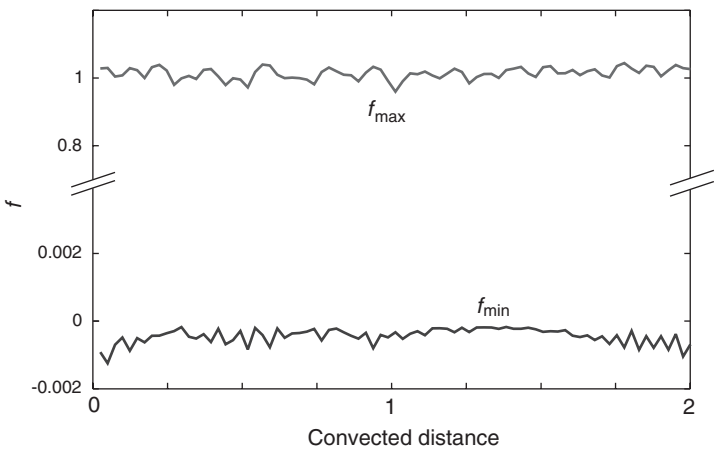

Figure 5. Evolution of minimum and maximum f value during advection ($Cr_{\max} = 0.95$).

A series of similar runs with different step sizes is done in order to asses the accuracy of the method in relation to the maximum Courant number. In Figure 6 the L_1 and the L_2 norms of the error at the end of the advection are shown. These norms are defined as

$$E_1 = \int_V |f_h - f^{\text{ref}}| \, \mathrm{d}V \Big/ \int_V |f^{\text{ref}}| \, \mathrm{d}V$$
$$E_2 = \sqrt{\int_V (f_h - f^{\text{ref}})^2 \, \mathrm{d}V \Big/ \int_V (f^{\text{ref}})^2 \, \mathrm{d}V} \tag{19}$$

Also shown in Figure 6 are these error norms for the 2nd order method without the implicit terms. Inclusion of implicit terms according to Equation (13) extends the stability region by approximately 30%.

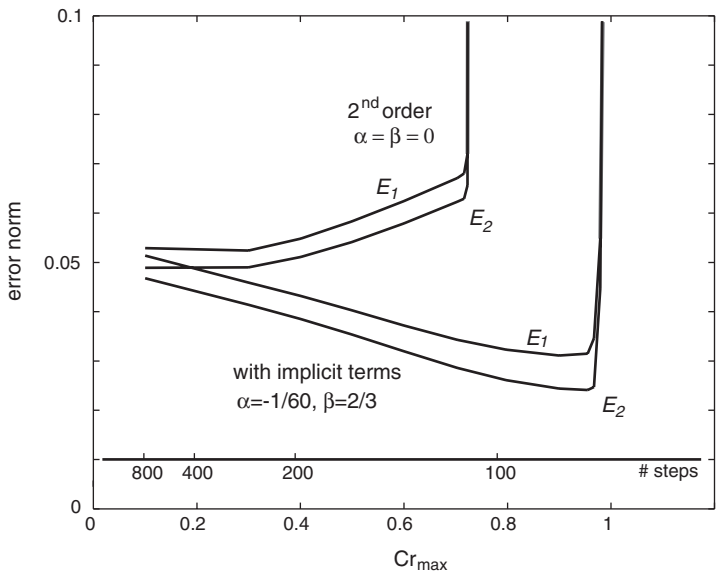

Figure 6. Error of the final distribution as function of the maximum Courant number.

4.2. *A non-uniform velocity field*

To demonstrate pure advection in a varying velocity field, the simulation of advection of a Gaussian bump is repeated with velocities defined as

$$\begin{Bmatrix} u \\ v \end{Bmatrix} = \begin{Bmatrix} 1 + \frac{1}{2}\cos \pi(x-1) \\ \frac{\pi y}{2} \sin \pi(x-1) \end{Bmatrix}, \quad \frac{1}{2} < x < \frac{3}{2}; \quad \begin{Bmatrix} 1 \\ 0 \end{Bmatrix} \quad \text{elsewhere} \tag{20}$$

This is a divergence free velocity field. In order to avoid spurious inflow from the sides, the boundaries are adapted to follow the stream lines.

A distance of 2 is covered in 93 steps. The maximum Courant number in any element is again 0.95. The resulting distribution is shown in Figure 7.

4.3. *A sharp front*

In these calculations the performance of the method in the presence of a sharp front is shown. The initial distribution is $f(x,0) = 0$. At the inflow boundary a condition $f_0(y) = 0, y < -0.053$; $f_0(y) = 1$ elsewhere is prescribed. The result after 85 steps ($Cr_{\max} = 0.92$) is shown in Figure 8. The front is typically smeared out over 3 elements. Loss of monotonicity is visible as a slight Gibbs effect.

5. CONCLUSIONS

We have presented a second order discontinuous Galerkin method for advection of element data. The data to be convected are discontinuous across element boundaries.

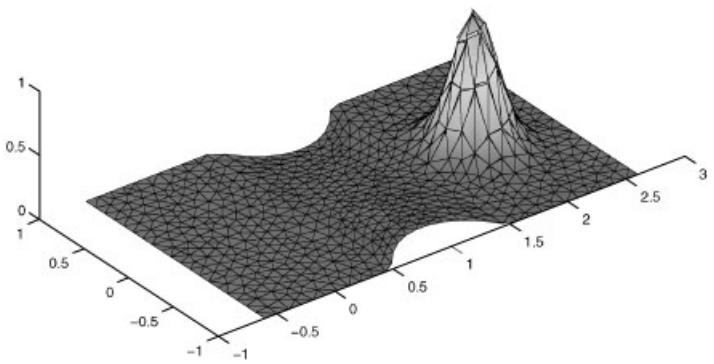

Figure 7. Advection of a Gaussian bump in a non-uniform velocity field, final distribution ($Cr_{\max} = 0.95$).

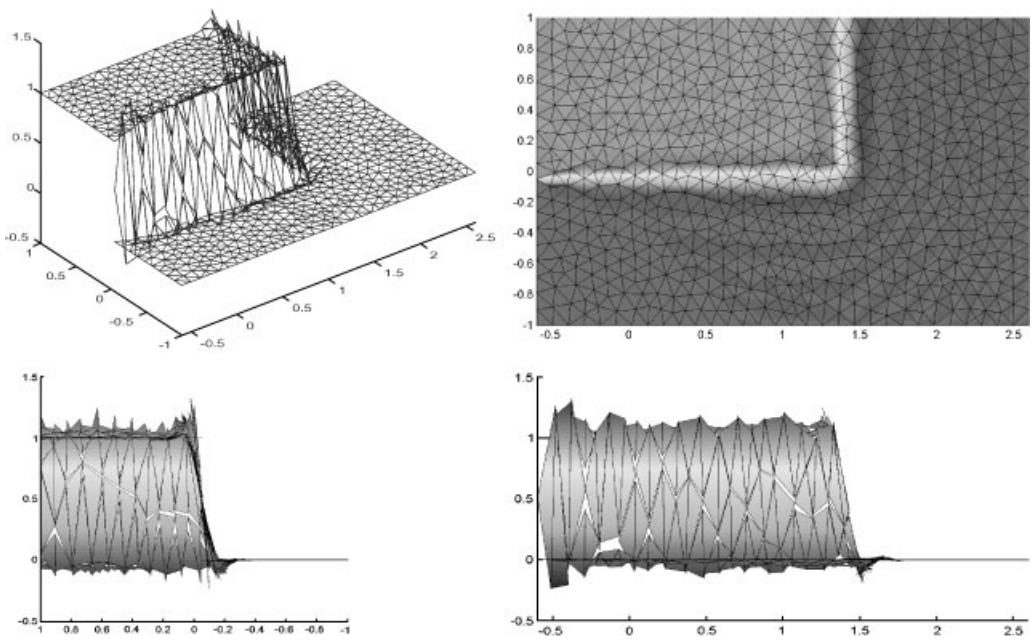

Figure 8. Advection of a sharp front ($Cr_{\max} = 0.92$).

A discretization is shown based on a second order Taylor expansion of the advection equation. This discretization results in an advection scheme which is stable for Courant numbers up to 0.7 in an unstructured mesh of triangular elements.

In order to extend the stability region of the scheme, the discretized equations are enriched with selective implicit terms. The result is an explicit and local scheme, which is stable and accurate for Courant numbers up to 0.95.

REFERENCES

1. Benson DJ. An efficient, accurate simple ALE method for nonlinear finite element programs. *Computational Methods in Applied Mechanics and Engineering* 1989; **72**:305–350.
2. Liu WK, Chang H, Chen JS, Belytschko T. Arbitrary Lagrangian-Eulerian Petrov-Galerkin finite elements for nonlinear continua. *Computational Methods in Applied Mechanics and Engineering* 1988; **68**:259–310.
3. Huétink J, Vreede PT, Van der Lugt J. Progress in mixed Euler-Lagrange FE simulation of forming processes. *International Journal for Numerical Methods in Engineering* 1990; **30**:1441–1457.
4. Siegel P, Mosé R, Ackerer Ph. Solution of the advection-diffusion equation using a combination of discontinuous and mixed finite elements. *International Journal for Numerical Methods in Fluids* 1997; **24**:595–613.
5. Cockburn BW. Devising discontinuous Galerkin methods for non-linear hyperbolic conservation laws. *Journal of Computational and Applied Mathematics* 2001; **128**:187–204.
6. Baumann CE, Oden JT. An adaptive order discontinuous Galerkin method for the solution of the Euler equations of gas dynamics. *International Journal for Numerical Methods in Engineering* 2000; **47**:61–73.
7. Lomtev I, Karniadakis GEM. A discontinuous Galerkin method for the Navier-Stokes equations. *International Journal for Numerical Methods in Fluids* 1999; **29**:587–603.
8. Fortin M, Fortin A. A new approach for the FEM simulation of viscoelastic flows. *Journal of Non-Newtonian Fluid Mechanics* 1989; **32**:295–310.
9. Pichelin E, Coupez T. Finite element solution of the 3D mold filling problem for viscous incompressible fluid. *Computational Methods in Applied Mechanics and Engineering* 1998; **163**:359–371.
10. Lesaint P, Raviart PA. On a finite element method for solving the neutron transport equation. In *Mathematical Aspects of Finite Elements in Partial Differential Equations*, de Boor C (ed). 1974; 89–123.
11. Oñate E. Derivation of stabilized equations for numerical solution of advective-diffusive transport and fluid flow problems. *Computational Methods in Applied Mechanics and Engineering* 1998; **151**:233–265.
12. de Sampaio PAB, Coutinho ALGA. A natural derivation of discontinuity capturing operator for advection-diffusion problems. *Computational Methods in Applied Mechanics and Engineering* 2001; **190**:6291–6308.

